**Figure S1.** Ratios between rate constants of several species of atmospheric interest with OH and their photoabsorption cross-sections at 185 nm (black markers) and ratios between 185 nm-photon (F185) and OH exposures for OFR185 (blue). The former are also equal to F185 exposure/OH exposure at which photons at 185 nm and OH consume species equally. Ratios between 185 nm photon and OH exposures in typical OFR cases are shown by markers. The reaction of the considered species with OH is preponderant over photolysis at 185 nm at a certain value of F185 exposure/OH exposure, when this value is located on the left of the considered species' black marker, as the turquoise solid arrow on the top indicates. The reverse is true when this value is on the right, as the carmine solid arrow on the top indicates.
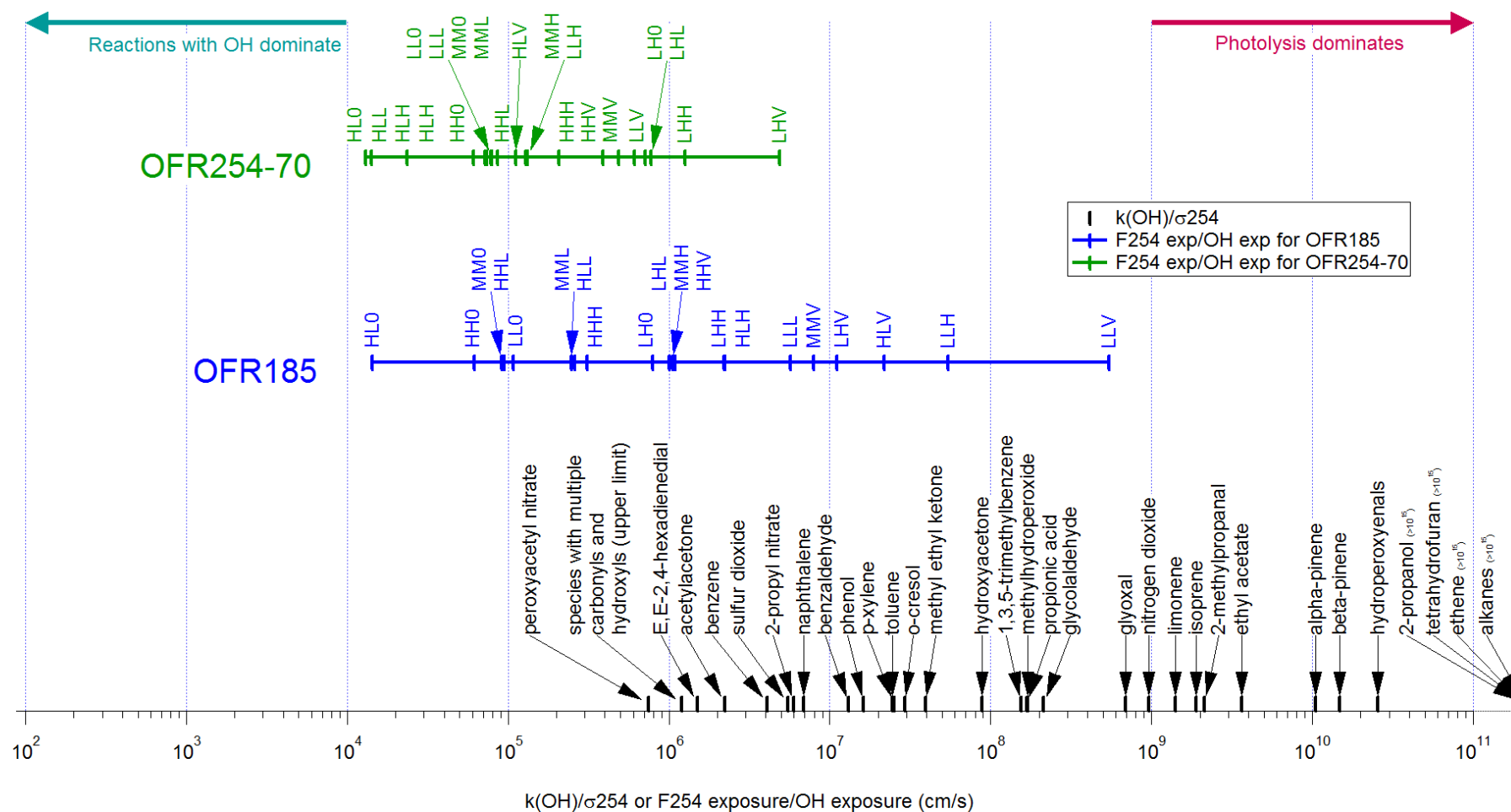
Figure S2. Same as Fig. S1, but for ratios of rate constants with OH and photoabsorption cross-sections at 254 nm and F254 exposure/OH exposure for OFR185 and OFR254-70.
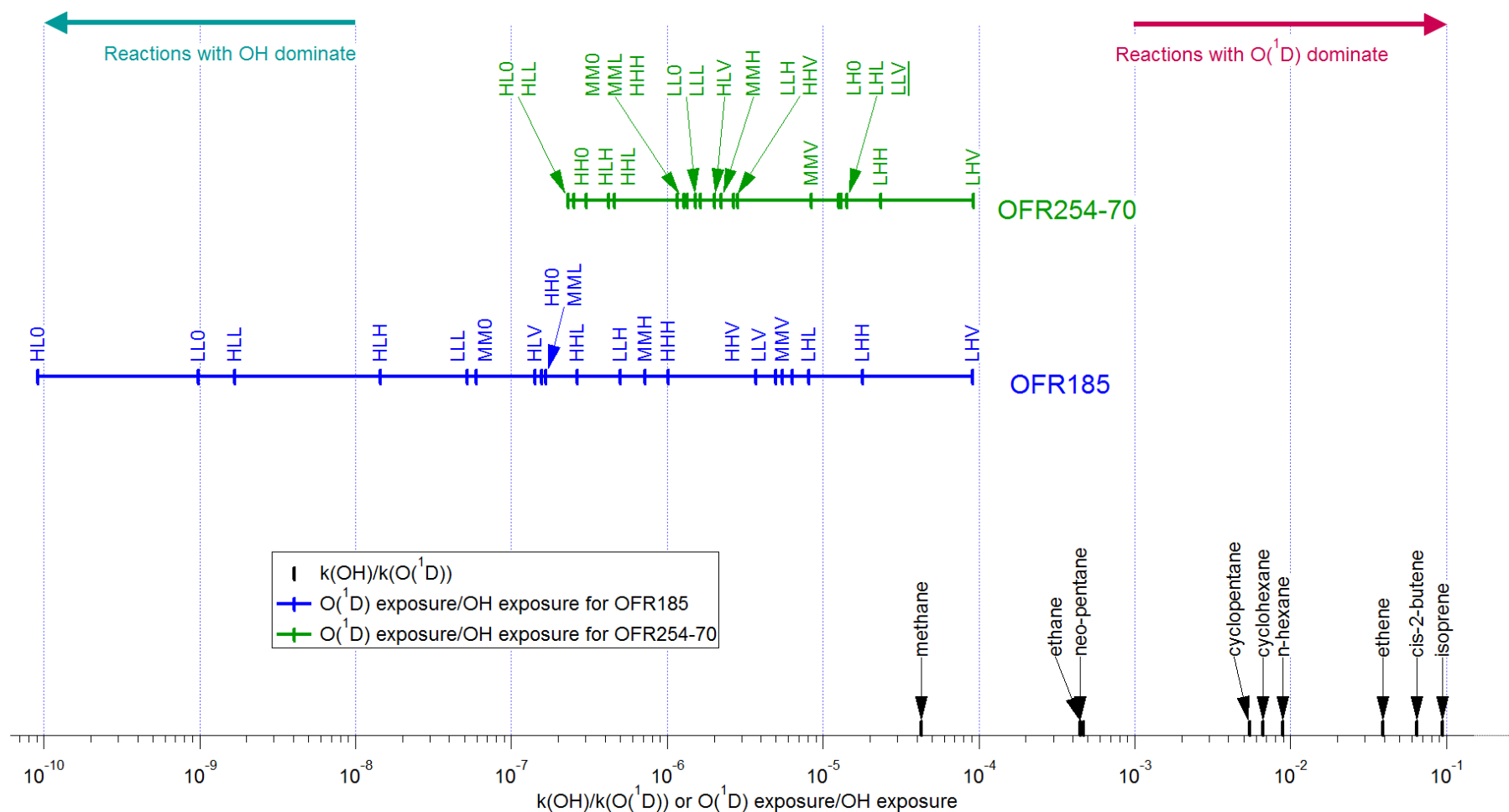
Figure S3. Same as Fig. S1, but for ratios of rate constants with OH and O(^{1}D) and O(^{1}D) exposure/OH exposure for OFR185 and OFR254-70.
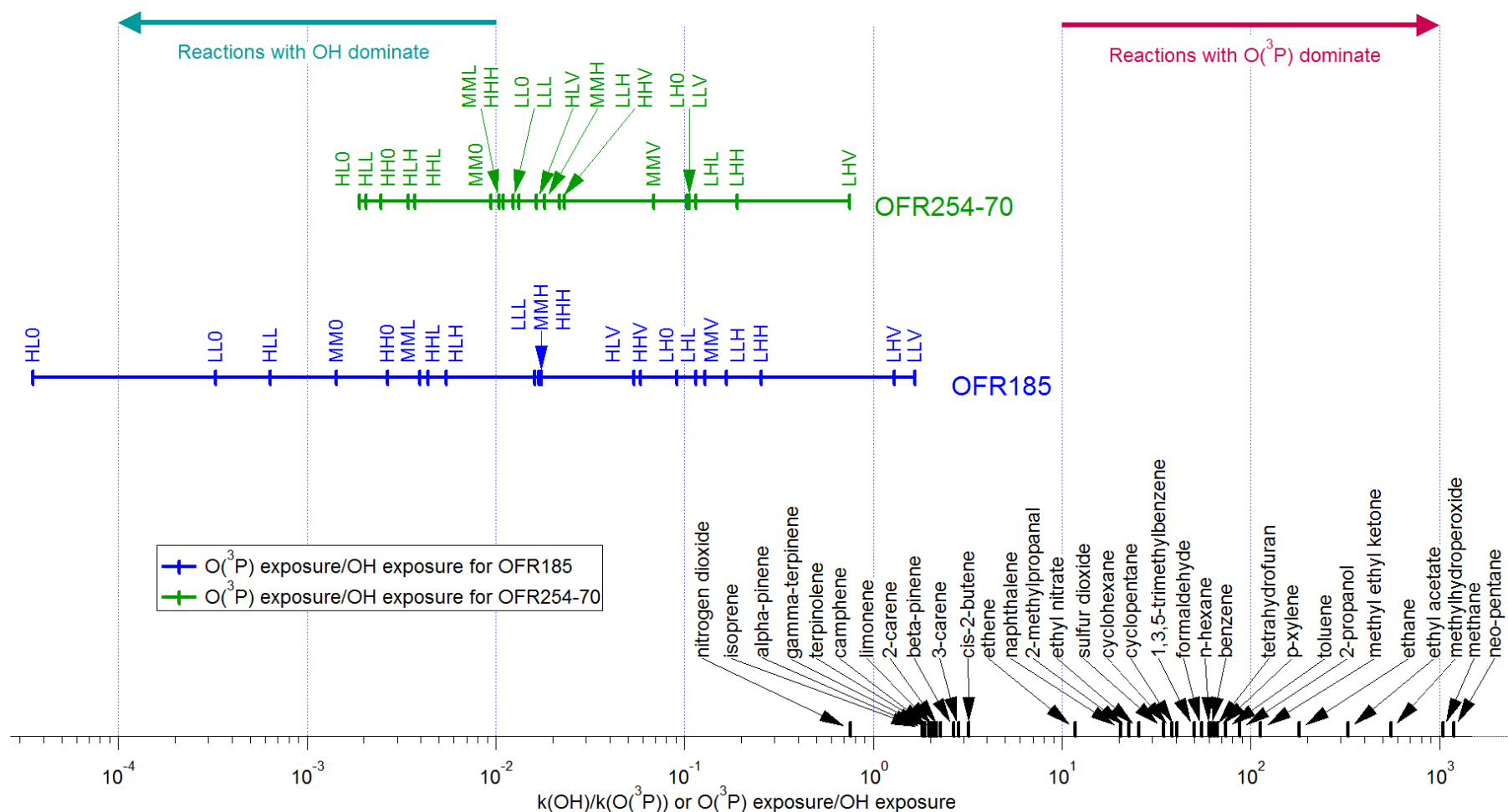
Figure S4. Same as Fig. S1, but for ratios of rate constants with OH and O(^{3}P) and O(^{3}P) exposure/OH exposure for OFR185 and OFR254-70.
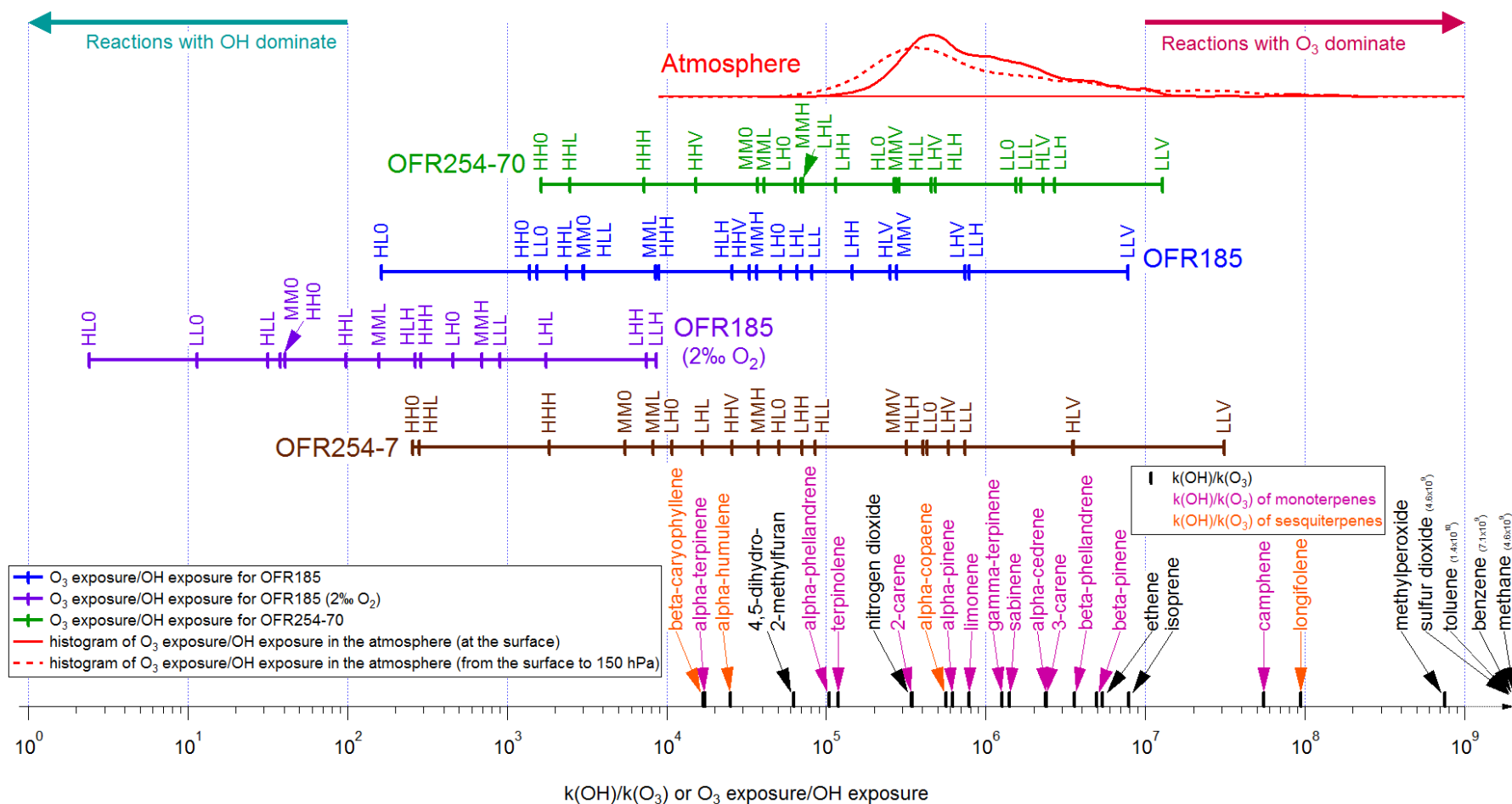
Figure S5. Same as Fig. S1, but for ratios of rate constants with OH and O₃ of species of atmospheric interest and O₃ exposure/OH exposure for OFR185 (blue), OFR185 with 0.2% O₂ (purple), OFR254-70 (dark green), and OFR254-7 (brown), and in the atmosphere (red).

Species names corresponding to ratios between rate constants of OH and of O₃ with monoterpenes, sesquiterpenes, and other species are in magenta, dark orange, and black, respectively. O₃ exposure/OH exposure at the Earth's surface (solid line) and throughout the column from the surface to a height with a pressure of 150 hPa (dashed line) in the atmosphere are shown by histograms, as simulated by the GISS ModelE2.
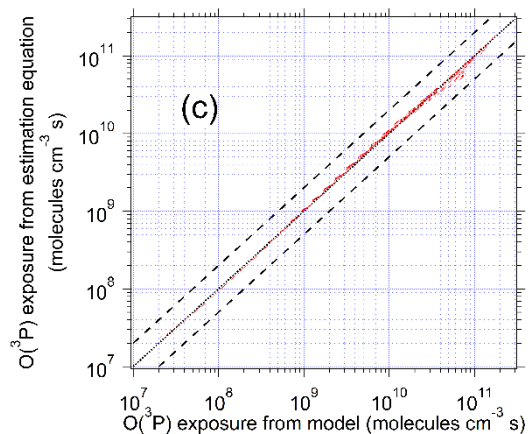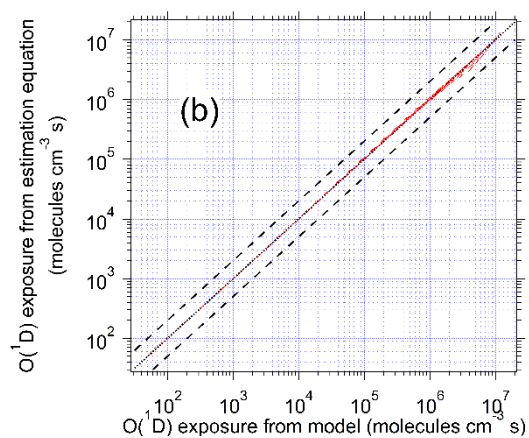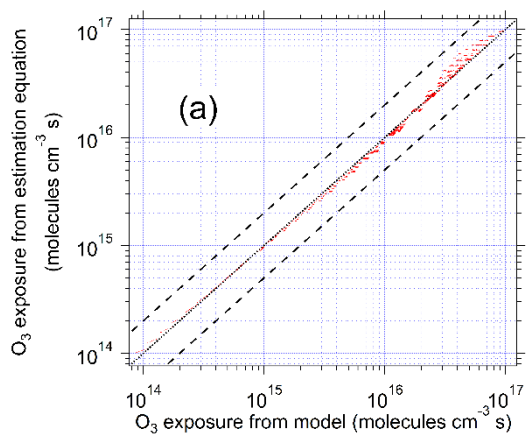
OFR185   OFR254
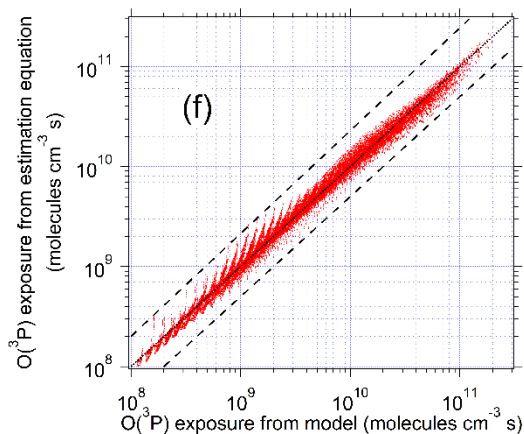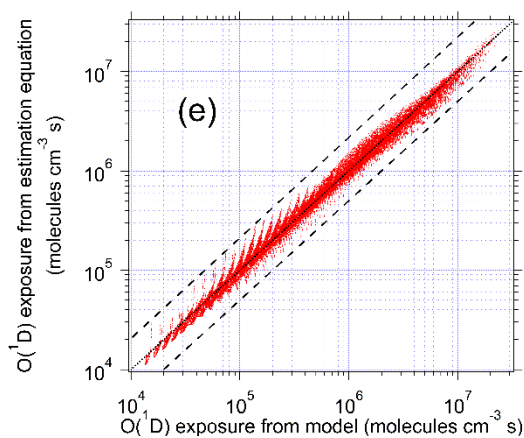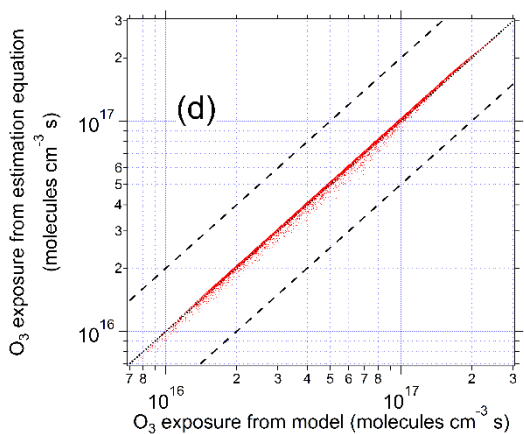
OFR185
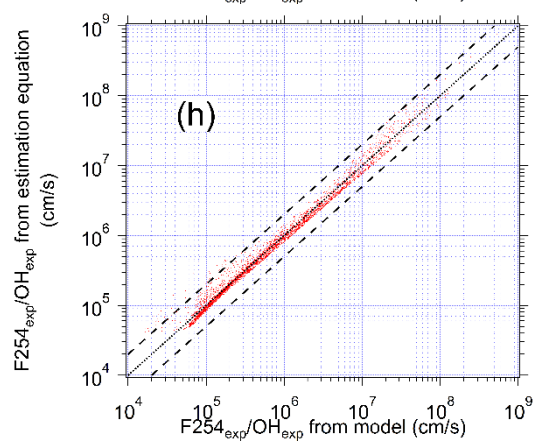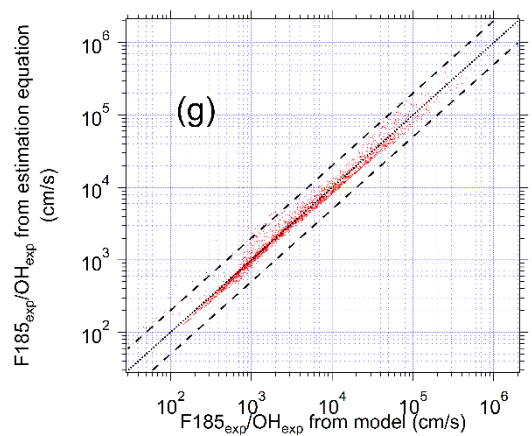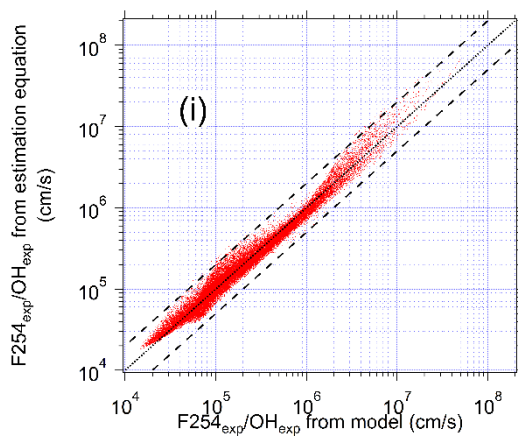
OFR254

OFR185
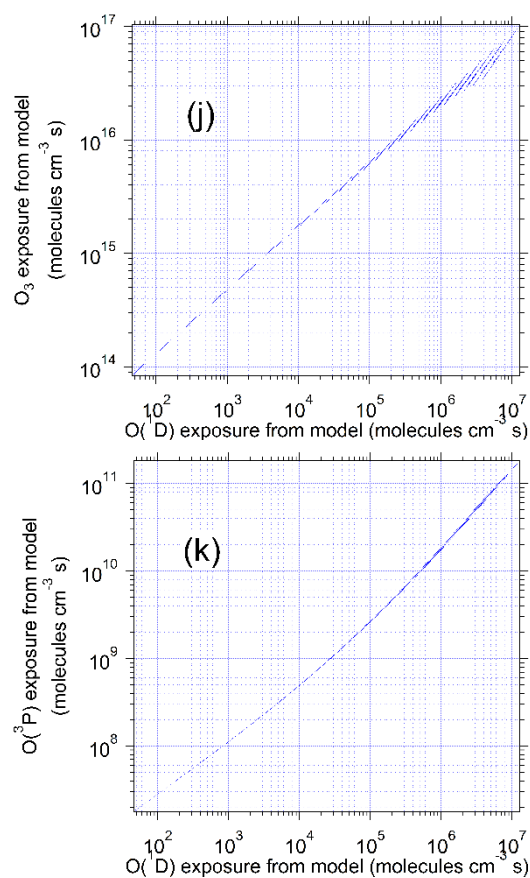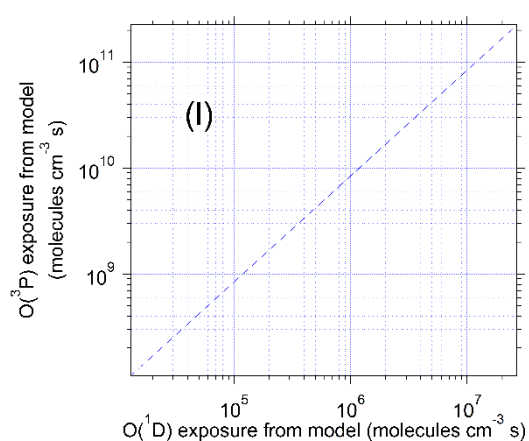
OFR254

Figure S6. O_3, $O(^1D)$, and $O(^3P)$ exposures and ratios of F185 and F254 exposures to OH exposure from estimation equations vs. those from the model for (a–c, g, h) OFR185 and (d–f, i) OFR254. 1:1 (dotted), 1:2, and 2:1 (dashed) lines are shown in (a–i) to facilitate comparison. Scatter plots between modeled exposures for (j, k) OFR185 and (l) OFR254 are also shown.

Table S1. Photoabsorption cross-sections (in cm^2 molecule^{-1}) of several species of atmospheric interest at 185 and 254 nm and rate constants (in cm^3 molecule^{-1} s^{-1}) of these species with OH at room temperature (298 K).

| Species	σ(185)	Ref	σ(254)	Ref	k(OH)	Ref
isoprene	1.28E-17	(Keller-Rudek et al., 2015)	5.28E-20	(Keller-Rudek et al., 2015)	1.00E-10	(Atkinson and Arey, 2003)
α-pinene	1.27E-17	(Keller-Rudek et al., 2015)	~5E-21	(Keller-Rudek et al., 2015)[*1]	5.23E-11	(Atkinson and Arey, 2003)
β-pinene	2.25E-17	(Keller-Rudek et al., 2015)	~5E-21	(Keller-Rudek et al., 2015)[*2]	7.43E-11	(Atkinson and Arey, 2003)
limonene	4.58E-17	(Keller-Rudek et al., 2015)	1.16E-19	(Keller-Rudek et al., 2015)	1.64E-10	(Atkinson and Arey, 2003)
sulfur dioxide	3.47E-18	(Keller-Rudek et al., 2015)	1.67E-19	(Keller-Rudek et al., 2015)	9.20E-13	(Sander et al., 2011)
nitrogen dioxide	6.88E-18	(Keller-Rudek et al., 2015)	1.05E-20	(Keller-Rudek et al., 2015)	1.01E-11	(Sander et al., 2011)
benzene	2.68E-17	(Keller-Rudek et al., 2015)	3.00E-19	(Keller-Rudek et al., 2015)	1.22E-12	(Atkinson and Arey, 2003)
toluene	1.52E-16	(Keller-Rudek et al., 2015)	2.29E-19	(Keller-Rudek et al., 2015)	5.63E-12	(Atkinson and Arey, 2003)
benzaldehyde	~5.3E-17	this work[*3]	9.20E-19	(Keller-Rudek et al., 2015)	1.20E-11	(Trost et al., 1997)
o-cresol	~1.3E-16	this work[*3]	1.43E-18	(Keller-Rudek et al., 2015)	4.20E-11	(Trost et al., 1997)
phenol	~1.1E-16	this work[*3]	1.63E-18	(Keller-Rudek et al., 2015)	2.63E-11	(Atkinson and Arey, 2003)
p-xylene	1.34E-16	(Keller-Rudek et al., 2015)	5.70E-19	(Keller-Rudek et al., 2015)	1.43E-11	(Atkinson and Arey, 2003)
1,3,5-trimethylbenzene	6.96E-17	(Keller-Rudek et al., 2015)	3.68E-19	(Keller-Rudek et al., 2015)	5.67E-11	(Atkinson and Arey, 2003)
naphthalene	1.20E-17	(Halasinski et al., 2005)	3.33E-18	(Ferguson et al., 1957)	2.30E-11	(Atkinson and Arey, 2003)
methylhydroperoxide	~9E-19	(Keller-Rudek et al., 2015)[*4]	3.23E-20	(Keller-Rudek et al., 2015)	3.80E-12	(Sander et al., 2011)
hydroperoxyenals	N/A	N/A	3.23E-20	(Keller-Rudek et al., 2015)[*5]	~5.1E-11	(Wolfe et al., 2012)[*6]
E,E-2,4-hexadienedial	N/A	N/A	3.32E-17	(Keller-Rudek et al., 2015)[*7]	~5E-11	(Ziemann and Atkinson, 2012)[*8]
acetylacetone	N/A	N/A	4.00E-17	(Messaadia et al., 2015)	8.89E-11	(Messaadia et al., 2015)
species with multiple carbonyls and hydroxyls	N/A	N/A	~5E-17[*9]	(Foster, 1969)	~6E-12	(Atkinson and Arey, 2003)[*10]
2-propanol	2.16E-18	(Keller-Rudek et al., 2015)	0	N/A	5.80E-12	(Atkinson and Arey, 2003)
glyoxal	4.80E-19	(Keller-Rudek et al., 2015)[*11]	1.59E-20	(Keller-Rudek et al., 2015)	1.10E-11	(Atkinson and Arey, 2003)
2-methylpropanal	5.71E-18	(Keller-Rudek et al., 2015)	1.22E-20	(Keller-Rudek et al., 2015)	2.60E-11	(Atkinson and Arey, 2003)
glycolaldehyde	3.85E-18	(Keller-Rudek et al., 2015)	3.76E-20	(Keller-Rudek et al., 2015)	8.00E-12	(Ammann et al., 2015)
methyl ethyl ketone	1.31E-18	(Keller-Rudek et al., 2015)	3.09E-20	(Keller-Rudek et al., 2015)	1.22E-12	(Atkinson and Arey, 2003)
hydroxyacetone	5.40E-18	(Keller-Rudek et al., 2015)	5.07E-20	(Keller-Rudek et al., 2015)	4.50E-12	(Ammann et al., 2015)
ethyl acetate	4.21E-19	(Keller-Rudek et al., 2015)	5.00E-22	(Keller-Rudek et al., 2015)[*12]	1.82E-12	(El Boudali et al., 1996)

propionic acid	7.25E-19	(Keller-Rudek et al., 2015)	7.11E-21	(Keller-Rudek et al., 2015)	1.20E-12	(Ammann et al., 2015)
pyruvic acid	N/A	N/A	1.61E-20	(Keller-Rudek et al., 2015)	1.20E-13	(Mellouki and Mu, 2003)
tetrahydrofuran	2.27E-18	(Keller-Rudek et al., 2015)	0	N/A	1.50E-11	(Atkinson, 1986)
2-propyl nitrate	1.79E-17	(Keller-Rudek et al., 2015)	4.86E-20	(Keller-Rudek et al., 2015)	2.90E-13	(Atkinson and Arey, 2003)
peroxyacetyl nitrate	6.20E-18	(Sander et al., 2011)[*13]	1.00E-19	(Sander et al., 2011)	7.50E-14	(Tsalkani et al., 1988)
ethene	1.87E-19	(Keller-Rudek et al., 2015)	0	N/A	8.52E-12	(Atkinson and Arey, 2003)
alkanes	0	N/A	0	N/A	~1E-12	(Atkinson and Arey, 2003)

*1: approximate average value between 245 and 250 nm

*2: approximate average value between 245 and 250 nm

*3: estimate based on quantum chemical calculations. See details below.

*4: extrapolation from the data between 210 and 280 nm, whose logarithm manifests a good linear wavelength-dependence

*5: value of a proxy, methylhydroperoxide, as the proxy used in Wolfe et al. (2012), E-2-hexanal, does not contain a hydroperoxy group and hence has little absorption at 254 nm.

*6: value of a proxy, C_6-hydroperoxyenal

*7: value at 248 nm

*8: estimated according to quantitative structure-activity relationship in Ziemann and Atkinson (2012)

*9: upper limit estimated according to relevant data in Foster (1969)

*10: typical value of saturated ketones

*11: value at 193 nm

*12: value at 252 nm

*13: linear extrapolation from the data between 196–206 nm

Table S2. Rate constants (in cm^3 molecule^{-1} s^{-1}) of several species of atmospheric interest with $O(^1D)$, $O(^3P)$, and OH at room temperature (298 K).

Species	k(O(^{1}D))	Ref	k(O(^{3}P))	Ref	k(OH)	Ref
sulfur dioxide	N/A	N/A	2.67E-14	(Atkinson et al., 1997)	9.19E-13	(Sander et al., 2011)
nitrogen dioxide	N/A	N/A	1.34E-11	(Sander et al., 2011)	1.01E-11	(Sander et al., 2011)
methane	1.50E-10	(Ammann et al., 2015)	6.12E-18	(Cohen and Westberg, 1991)	6.40E-15	(Atkinson and Arey, 2003)
ethane	5.30E-10	(Michaud et al., 1974)	1.38E-15	(Cohen and Westberg, 1991)	2.48E-13	(Atkinson and Arey, 2003)
neo-pentane	1.84E-09	(Pitts et al., 1974)	6.91E-16	(Cohen and Westberg, 1991)	8.25E-13	(Atkinson and Arey, 2003)
cyclopentane	9.05E-10	(Michaud et al., 1974)	1.23E-13	(Cohen and Westberg, 1991)	4.97E-12	(Atkinson and Arey, 2003)
n-hexane	5.80E-10	(Dillon et al., 2008)	8.69E-14	(Cohen and Westberg, 1991)	5.20E-12	(Atkinson and Arey, 2003)
cyclohexane	1.05E-09	(Michaud et al., 1974)	1.83E-13	(Cohen and Westberg, 1991)	6.97E-12	(Atkinson and Arey, 2003)
ethene	2.19E-10	(Kajimoto and Fueno, 1979)	7.25E-13	(Cvetanović, 1987)	8.52E-12	(Atkinson and Arey, 2003)
cis-2-butene	8.70E-10	(Kajimoto and Fueno, 1979)	1.76E-11	(Cvetanović, 1987)	5.64E-11	(Atkinson and Arey, 2003)
methylhydroperoxide	N/A	N/A	1.00E-14	(Baulch et al., 1994)	5.50E-12	(Atkinson and Arey, 2003)
benzene	N/A	N/A	1.99E-14	(Cvetanović, 1987)	1.22E-12	(Atkinson and Arey, 2003)
toluene	N/A	N/A	7.63E-14	(Baulch et al., 1994)	5.63E-12	(Atkinson and Arey, 2003)
p-xylene	N/A	N/A	2.15E-13	(Baulch et al., 1994)	1.43E-11	(Atkinson and Arey, 2003)
1,3,5-trimethylbenzene	N/A	N/A	1.13E-12	(Cvetanović, 1987)	5.67E-11	(Atkinson and Arey, 2003)
naphthalene	N/A	N/A	1.13E-12	(Frerichs et al., 1990)	2.30E-11	(Atkinson and Arey, 2003)
isoprene	1.06E-09	(Kajimoto and Fueno, 1979)	5.52E-11	(Cvetanović, 1987)	1.00E-10	(Atkinson and Arey, 2003)
α-pinene	N/A	N/A	2.79E-11	(Luo et al., 1996)	5.23E-11	(Atkinson and Arey, 2003)
β-pinene	N/A	N/A	2.80E-11	(Luo et al., 1996)	7.43E-11	(Atkinson and Arey, 2003)
3-carene	N/A	N/A	3.12E-11	(Luo et al., 1996)	8.80E-11	(Atkinson and Arey, 2003)
2-carene	N/A	N/A	3.54E-11	(Luo et al., 1996)	8.00E-11	(Atkinson and Arey, 2003)
camphene	N/A	N/A	2.60E-11	(Luo et al., 1996)	5.30E-11	(Atkinson and Arey, 2003)
limonene	N/A	N/A	7.60E-11	(Luo et al., 1996)	1.64E-10	(Atkinson and Arey, 2003)
γ-terpinene	N/A	N/A	9.00E-11	(Luo et al., 1996)	1.77E-10	(Atkinson and Arey, 2003)
terpinolene	N/A	N/A	1.07E-10	(Luo et al., 1996)	2.25E-10	(Atkinson and Arey, 2003)
2-propanol	N/A	N/A	6.64E-14	(Herron, 1988)	5.80E-12	(Atkinson and Arey, 2003)
2-methylpropanal	N/A	N/A	1.15E-12	(Herron, 1988)	2.60E-11	(Atkinson and Arey, 2003)

methyl ethyl ketone	N/A	N/A	1.09E-14	(Herron, 1988)	1.22E-12	(Atkinson and Arey, 2003)
ethyl acetate	N/A	N/A	5.59E-15	(Herron, 1988)	1.82E-12	(El Boudali et al., 1996)
tetrahydrofuran	N/A	N/A	2.36E-13	(Herron, 1988)	1.50E-11	(Atkinson, 1986)
ethyl nitrate	N/A	N/A	7.02E-15	(Salter and Thrush, 1977)	1.80E-13	(Atkinson and Arey, 2003)
formaldehyde	N/A	N/A	1.70E-13	(Herron, 1988)	9.37E-12	(Atkinson and Arey, 2003)

Table S3. Rate constants (in cm^3 $molecule^{-1}$ s^{-1}) of several species of atmospheric interest with O_3, and OH at room temperature (298 K).

Species	k(OH)	Ref	k(O$_3$)	Ref
isoprene	1.00E-10	(Atkinson and Arey, 2003)	1.27E-17	(Atkinson and Arey, 2003)
camphene	5.30E-11	(Atkinson and Arey, 2003)	9.60E-19	(Atkinson and Arey, 2003)
2-carene	8.00E-11	(Atkinson and Arey, 2003)	2.30E-16	(Atkinson and Arey, 2003)
3-carene	8.80E-11	(Atkinson and Arey, 2003)	3.70E-17	(Atkinson and Arey, 2003)
limonene	1.64E-10	(Atkinson and Arey, 2003)	2.10E-16	(Atkinson and Arey, 2003)
α-phellandrene	3.13E-10	(Atkinson and Arey, 2003)	3.00E-15	(Atkinson and Arey, 2003)
β-phellandrene	1.68E-10	(Atkinson and Arey, 2003)	4.70E-17	(Atkinson and Arey, 2003)
α-pinene	5.23E-11	(Atkinson and Arey, 2003)	8.40E-17	(Atkinson and Arey, 2003)
β-pinene	7.43E-11	(Atkinson and Arey, 2003)	1.50E-17	(Atkinson and Arey, 2003)
sabinene	1.17E-10	(Atkinson and Arey, 2003)	8.30E-17	(Atkinson and Arey, 2003)
α-terpinene	3.63E-10	(Atkinson and Arey, 2003)	2.10E-14	(Atkinson and Arey, 2003)
γ-terpinene	1.77E-10	(Atkinson and Arey, 2003)	1.40E-16	(Atkinson and Arey, 2003)
terpinolene	2.25E-10	(Atkinson and Arey, 2003)	1.90E-15	(Atkinson and Arey, 2003)
α-cedrene	6.70E-11	(Atkinson and Arey, 2003)	2.80E-17	(Atkinson and Arey, 2003)
α-copaene	9.00E-11	(Atkinson and Arey, 2003)	1.60E-16	(Atkinson and Arey, 2003)
β-caryophyllene	1.97E-10	(Atkinson and Arey, 2003)	1.16E-14	(Atkinson and Arey, 2003)
α-humulene	2.93E-10	(Atkinson and Arey, 2003)	1.17E-14	(Atkinson and Arey, 2003)
longifolene	4.70E-11	(Atkinson and Arey, 2003)	5.00E-19	(Atkinson and Arey, 2003)
methane	6.40E-15	(Atkinson and Arey, 2003)	1.40E-24	(Schubert et al., 1956)
ethene	8.52E-12	(Atkinson and Arey, 2003)	1.59E-18	(Atkinson and Arey, 2003)
benzene	1.22E-12	(Atkinson and Arey, 2003)	1.72E-22	(Toby et al., 1985)
toluene	5.63E-12	(Atkinson and Arey, 2003)	3.90E-22	(Toby et al., 1985)
methylperoxide	5.50E-12	(Atkinson and Arey, 2003)	7.30E-21	(Chen and Wang, 2006)
4,5-dihydro-2-methylfuran	2.18E-10	(Atkinson and Arey, 2003)	3.49E-15	(Atkinson and Arey, 2003)
sulfur dioxide	9.20E-13	(Sander et al., 2011)	2.00E-22	(Sander et al., 2011)
nitrogen dioxide	1.01E-11	(Sander et al., 2011)	2.97E-17	(Sander et al., 2011)

Table S4. Summary of the previous studies using OFRs. In case of multiple experiments with a certain source in a certain study, only the most (low water mixing ratio and high external OH reactivity) and the least (high water mixing ratio and low external OH reactivity) pathological cases are shown. Source, external OH reactivity (Ext. OHR), OH exposure (OH exp.), and relative humidity (RH) in each experiment are collected from the literature. Exposure ratios and percentages of the rate of a type of reactions [r(X), X=185 nm photons, 254 nm photons, O(^{1}D), O(^{3}P), and O$_3$] in the sum of the rates of these reactions and those with OH [r(X)+r(OH)] are estimated by our model. Photolysis at 185 and 254 nm is considered as non-tropospheric reactions (NTR). An example of the improvement of study using OFR is also shown for comparison.

Study	Source type	Source mixing ratio (ppb)	Ext. OHR (s^{-1})	OH exp. (molec cm^{-3} s)	RH (%)	Examined species	F185 exp./OH exp. (cm/s)	r(185)/(r(185)+r(OH)) (%)	F254 exp./OH exp. (cm/s)	r(254)/(r(254)+r(OH)) (%)	$O(^1D)$ exp./OH exp. (%)	r($O(^1D)$)/(r($O(^1D)$)+r(OH)) (%)[*8]	$O(^3P)$ exp./OH exp.	r($O(^3P)$)/(r($O(^3P)$)+r(OH)) (%)	O_3 exp./OH exp.	r(O_3)/(r(O_3)+r(OH)) (%)[*9]	r(non-OH)/(r(total)) (%)	r(NTR)/(r(total)) (%)
Kang et al. 2011	α-pinene	39	49	2.8E+11	3	α-pinene			3.1E+06	0.03	7.7E-06	0.02	5.3E-02	2.88	1.8E+05	23.45	26.38	0.02
				2.3E+12	42				3.3E+05	0.00	6.0E-07	0.00	4.2E-03	0.23	1.7E+04	2.81	3.04	0.00
	m-xylene	170	94	2.4E+11	4	m-xylene			4.3E+06	8.47	1.0E-05	0.05	7.3E-02	0.13	2.1E+05	0.01	8.62	8.46
				2.4E+12	48				5.6E+05	1.21	8.4E-07	0.00	5.8E-03	0.01	1.4E+04	0.00	1.22	1.21
	p-xylene	180	62	2.1E+11	4	p-xylene			2.6E+06	9.58	6.7E-06	0.05	4.6E-02	0.06	2.5E+05	0.02	9.68	9.57
				1.6E+12	32				5.4E+05	2.11	1.0E-06	0.01	7.2E-03	0.01	2.6E+04	0.00	2.13	2.11
	mixture	*1	88	1.8E+11	3	α-pinene			5.8E+06	0.06	1.5E-05	0.03	1.0E-01	5.32	2.9E+05	32.40	37.81	0.04
						m-xylene				11.23		0.06		0.17		0.01	11.42	11.20
						p-xylene				18.88		0.10		0.14		0.02	19.05	18.84
				2.3E+12	44	α-pinene			5.6E+05	0.01	8.7E-07	0.00	6.0E-03	0.75	1.5E+04	2.41	3.13	0.01
						m-xylene				1.19		0.00		0.01		0.00	1.21	1.19
						p-xylene				2.17		0.01		0.01		0.00	2.19	2.17
Lambe et al. 2011	n-decane	330	87	1.6E+11	30	n-decane			1.7E+05	0.00	1.2E-06	0.12	8.6E-03	0.00	4.1E+05	0.00	0.12	0.00
		102	27	2.5E+12	40				1.5E+05	0.00	8.7E-07	0.09	6.0E-03	0.00	2.2E+04	0.00	0.09	0.00
	isoprene	330	792	1.6E+11	30	isoprene			2.2E+05	0.01	1.1E-06	0.00	7.9E-03	0.43	4.1E+05	4.95	5.36	0.01
				2.5E+12	40				1.3E+05	0.01	6.1E-07	0.00	4.2E-03	0.23	2.2E+04	0.28	0.52	0.01
	α-pinene	50	63	1.6E+11	30	α-pinene			1.3E+05	0.00	9.5E-07	0.00	6.6E-03	0.36	4.1E+05	40.73	41.10	0.00
				2.5E+12	40				2.0E+05	0.00	1.1E-06	0.00	7.9E-03	0.44	2.1E+04	3.43	3.87	0.00
	β-pinene	50	89	1.6E+11	30	β-pinene			1.8E+05	0.00	1.3E-06	0.00	8.7E-03	0.54	4.1E+05	7.61	8.07	0.00
				2.5E+12	40				2.4E+05	0.00	1.3E-06	0.00	9.3E-03	0.58	2.1E+04	0.41	0.99	0.00
	toluene	80	11	1.6E+11	30	toluene			5.4E+04	0.24	3.9E-07	0.01	2.7E-03	0.00	4.2E+05	0.00	0.25	0.24
				2.5E+12	40				1.2E+05	0.53	7.5E-07	0.01	5.2E-03	0.01	2.2E+04	0.00	0.55	0.53
	m-xylene	103	57	1.6E+11	30	m-xylene			1.2E+05	0.27	8.8E-07	0.00	6.1E-03	0.01	4.1E+05	0.02	0.30	0.27
		86	48	2.5E+12	40				1.7E+05	0.38	1.0E-06	0.00	7.1E-03	0.01	2.2E+04	0.00	0.40	0.38
	1,3,5-trimethyl-benzene	150	204	1.6E+11	30	1,3,5-trimethyl-benzene			3.9E+05	0.26	2.8E-06	0.00	1.9E-02	4.55	4.1E+05	0.01	4.80	0.25
		120	163	2.5E+12	40				3.7E+05	0.25	1.9E-06	0.00	1.3E-02	3.22	1.9E+04	0.00	3.45	0.24
Klems et al. 2015	dodecanoic acid	400	123[*4]	1.7E+09[*5]	3	dodecanoic acid			1.6E+07	0.36	5.2E-06	0.04	4.3E-02	0.06	1.5E+04	0.00	0.46	0.36
Tkacik et al. 2014	tunnel air	*2	~300	7.4E+10	42[*6]	toluene[*7]	9.8E+03	20.97	1.5E+06	5.86	2.5E-07	0.00	1.0E-02	0.01	1.8E+04	0.00	24.69	24.67
		*3	~100	2.4E+12	42[*6]		1.3E+03	3.48	1.5E+05	0.60	1.6E-07	0.00	2.7E-03	0.00	3.8E+03	0.00	4.04	4.04
FLAME-3	wood smoke			~250	2.5E+11[*5]	22[*6]	benzene[*7]	2.6E+04	36.31	4.4E+06	51.97	1.7E-06	0.14	4.1E-02	0.07	1.6E+05	0.00	62.32	62.25
						α-pinene[*7]		0.63		0.04		0.00		2.15		20.32	22.10	0.52
BEACHON	ambient air		~15	2.1E+12[*5]	63[*6]	α-pinene[*7]	8.8E+02	0.02	1.5E+05	0.00	1.3E-07	0.00	2.8E-03	0.15	6.3E+03	1.00	1.17	0.02
SOAS			~20	1.4E+12[*5]	83[*6]	isoprene[*7]	8.1E+02	0.01	1.5E+05	0.01	5.7E-08	0.00	1.4E-03	0.08	5.4E+03	0.07	0.16	0.02
CalNex			~25	8.8E+11[*5]	43[*6]	toluene[*7]	1.1E+03	2.85	2.0E+05	0.82	1.2E-07	0.00	3.1E-03	0.00	1.2E+04	0.00	3.63	3.62
Improvement for FLAME-3	wood smoke		~50	8.7E+11[*5]	22[*6]	benzene[*7]	3.8E+03	7.72	4.8E+05	10.53	6.2E-07	0.05	1.0E-02	0.02	2.2E+04	0.00	16.81	16.76
						α-pinene[*7]		0.09		0.00		0.00		0.53		3.38	3.96	0.09
Improvement for BEACHON	ambient air		~15	3.2E+12[*5]	92[*10]	α-pinene[*7]	7.5E+02	0.02	1.0E+05	0.00	6.3E-08	0.00	1.1E-03	0.06	3.2E+03	0.51	0.59	0.02

*1: 37 ppb α-pinene, 46 ppb m-xylene, and 47 ppb p-xylene

*2: 785 ppb NO_x, 1.9 ppm CO, and VOC of an OH reactivity of 49.7 s^{-1}, estimated from a linear CO-VOC relationship [VOC of 26.1 s^{-1} OH reactivity per ppm CO (Borbon et al., 2013)]

*3: 310 ppb NO_x, 0.2 ppm CO, and VOC of an OH reactivity of 5.2 s^{-1}, according to the same linear relationship

*4: estimated according to the rate constant of dodecane reported in Atkinson and Arey (2003)

*5: calculated by our model

*6: average value

*7: a typical species in source, not the only component

*8: rate constants of reactions of examined species with $O(^1D)$ that are not available are assumed to be 10^{-9} cm^3 molecule s^{-1}

*9: rate constants of reactions of n-decane and alkylbenzenes with O_3 are taken from their upper limits reported in Atkinson and Arey (2003)

*10: corresponding to a water vapor mixing ratio of 2.3%

Table S5. Absorption cross-sections at 185 and 254 nm for several atmospheric oxidation intermediates from Keller-Rudek et al. (2015), ambient photolysis rate constants from Hodzic et al. (2015), and photolysis percentages in OFR185 and OFR254-70 (under the condition of 70% relative humidity and 25 s^{-1} initial OHR$_{ext}$) and in the troposphere at an OH exposure equivalent to a photochemical age of 1 week (assuming an ambient OH concentration of 1.5x10^6 molecules cm^{-3}). "N/A" in the table stands for "not available".

Species	Cross-sections (cm^2)		Ambient photolysis rate constant (s^{-1})	Photolysis percentage		
	185 nm	254 nm		OFR185	OFR254-70	Ambient
acrolein	2.82E-17	7.00E-22	1.39E-06	4.1	0.002	57
methacrolein	6.77E-18	1.78E-21	1.34E-05	1.0	0.005	100
acetone	2.91E-18	3.01E-20	3.82E-07	1.1	0.083	21
biacetyl	1.46E-18	3.71E-20	2.29E-04	1.0	0.103	100
pyruvic acid	N/A	1.61E-20	1.03E-04	N/A	0.045	100
methyl vinyl ketone	N/A	2.41E-21	4.72E-06	N/A	0.007	94
methylglyoxal	N/A	2.76E-20	7.79E-05	N/A	0.076	100
hydroxyacetone	5.40E-18	5.07E-20	1.51E-06	1.9	0.140	60
2,4-dimethyl-3-pentanone	N/A	1.66E-20	8.30E-06	N/A	0.046	99
2-methylpropanal	5.71E-18	1.22E-20	3.80E-05	1.1	0.034	100
4-methyl-2-pentanone	N/A	2.75E-20	5.48E-06	N/A	0.076	96
5-methyl-2-hexanone	N/A	2.39E-20	4.34E-06	N/A	0.066	93
2-propyl nitrate	1.79E-17	4.86E-20	1.93E-06	3.7	0.135	69
crotonaldehyde	1.05E-17	2.80E-21	9.87E-06	1.6	0.008	100
acetaldehyde	7.83E-20	1.57E-20	3.51E-06	0.4	0.044	88
3-pentanone	N/A	3.00E-20	3.07E-06	N/A	0.083	84
methyl ethyl ketone	1.31E-18	3.09E-20	2.98E-06	0.9	0.086	83
propanal	1.42E-17	1.75E-20	1.30E-05	2.5	0.048	100
n-butanal	7.99E-18	1.45E-20	1.14E-05	1.5	0.040	100
n-pentanal	N/A	1.43E-20	1.63E-06	N/A	0.040	63

n-hexanal	N/A	1.14E-20	1.18E-05	N/A	0.032	100
1-butyl nitrate	1.81E-17	4.60E-20	1.71E-06	3.6	0.127	64
1-propyl nitrate	1.81E-17	4.40E-20	1.84E-06	3.6	0.122	67
ethyl nitrate	1.71E-17	4.10E-20	1.16E-06	3.4	0.114	50
methyl nitrate	2.10E-17	3.34E-20	7.27E-07	3.8	0.093	36
methylhydroperoxide	9.00E-19	3.23E-20	4.25E-06	0.9	0.089	92
glyoxal	4.80E-19	1.59E-20	4.72E-04	0.4	0.044	100
peroxyacetyl nitrate	6.20E-18	1.00E-19	6.24E-07	3.1	0.277	31
glycolaldehyde	3.85E-18	3.76E-20	6.82E-06	1.4	0.104	98
hydroxymethyl hydroperoxide	N/A	2.88E-20	3.90E-06	N/A	0.080	91

Table S6. Percentage of non-OH fate of α-pinene and toluene in the "corner" cases (highest and lowest water mixing ratio, lamp setting, and external OH reactivity) in OFR185, OFR254-70, and OFR254-7. The cases with 0 external OH reactivity actually show non-OH VOC consumption at external OH reactivity very close but not equal to 0.

Case	OFR185		OFR254-70		OFR254-7	
	α-pinene	toluene	α-pinene	toluene	α-pinene	toluene
LL0	0.4	0.1	81.9	0.1	55.7	0.0
L"L"0	1.5	0.3	65.7	0.1	32.3	0.1
LH0	13.9	2.4	19.9	0.4	4.6	0.2
HL0	0.0	0.0	44.0	0.0	12.9	0.0
H"L"0	0.1	0.0	21.4	0.0	4.2	0.0
HH0	0.6	0.2	0.6	0.0	0.1	0.0
LLV	95.1	77.4	97.4	0.6	98.9	2.8
L"L"V	93.6	71.9	94.0	0.9	97.1	4.2
LHV	68.2	24.0	63.7	3.0	72.1	8.8
HLV	40.6	12.2	87.2	0.1	91.3	0.3
H"L"V	36.6	10.6	68.4	0.1	73.0	0.4
HHV	11.2	3.1	5.6	0.1	11.1	0.7

Table S7. Photoabsorption cross-sections (in cm^2 molecule^{-1}) of several surrogate SOA components at 185 and 254 nm and number of e-fold decays of photolysis of these species in the case of high H_2O, high UV, and high OHR_{ext} (Case HHH). Numbers of e-fold decays in OFR no less than 0.1 are in bold, and those no less than 1 are highlighted in gray cell. Ambient e-fold decay numbers corresponding to the same photochemical age as Case HHH are also shown for comparison.

Species	σ(185)	Ref	σ(254)	Ref	Number of e-fold decay of photolysis		
					185 nm	254 nm	Ambient
sulfuric acid	<1E-19	(Keller-Rudek et al., 2015)	<1E-21	(Keller-Rudek et al., 2015)	<1.8E-03	<1.5E-03	0
nitric acid	1.71E-17	(Keller-Rudek et al., 2015)	1.95E-20	(Keller-Rudek et al., 2015)	**0.31**	2.9E-02	7.1
benzaldehyde	5.30E-17	this work[*1]	9.20E-19	(Keller-Rudek et al., 2015)	**0.95**	**1.4**	7700
o-cresol	1.30E-16	this work[*1]	1.43E-18	(Keller-Rudek et al., 2015)	**2.3**	**2.1**	0
phenol	1.10E-16	this work[*1]	1.63E-18	(Keller-Rudek et al., 2015)	**2.0**	**2.4**	0
naphthalene	1.20E-17	(Halasinski et al., 2005)	3.33E-18	(Ferguson et al., 1957)	**0.22**	**5.0**	0
methylhydroperoxide	9.00E-19	(Keller-Rudek et al., 2015)[*2]	3.23E-20	(Keller-Rudek et al., 2015)	1.6E-02	4.8E-02	57
2-propanol	2.16E-18	(Keller-Rudek et al., 2015)	0	N/A	3.9E-02	0	0
glyoxal	4.80E-19	(Keller-Rudek et al., 2015)[*3]	1.59E-20	(Keller-Rudek et al., 2015)	8.6E-03	2.4E-02	640
2-methylpropanal	5.71E-18	(Keller-Rudek et al., 2015)	1.22E-20	(Keller-Rudek et al., 2015)	**0.10**	1.8E-02	510
glycolaldehyde	3.85E-18	(Keller-Rudek et al., 2015)	3.76E-20	(Keller-Rudek et al., 2015)	6.9E-02	5.6E-02	91
methyl ethyl ketone	1.31E-18	(Keller-Rudek et al., 2015)	3.09E-20	(Keller-Rudek et al., 2015)	2.4E-02	4.6E-02	40
hydroxyacetone	5.40E-18	(Keller-Rudek et al., 2015)	5.07E-20	(Keller-Rudek et al., 2015)	9.7E-02	7.6E-02	34
ethyl acetate	4.21E-19	(Keller-Rudek et al., 2015)	5.00E-22	(Keller-Rudek et al., 2015)[*4]	7.6E-03	7.5E-04	0
pentanoic acid	1.44E-18	(Keller-Rudek et al., 2015)	3.00E-21	(Keller-Rudek et al., 2015)	2.6E-02	4.5E-03	0
tetrahydrofuran	2.27E-18	(Keller-Rudek et al., 2015)	0	N/A	4.1E-02	0	0
alkanes	0	N/A	0	N/A	0	0	0
2-propyl nitrate	1.79E-17	(Keller-Rudek et al., 2015)	4.86E-20	(Keller-Rudek et al., 2015)	**0.32**	7.3E-02	26
peroxyacetyl nitrate	6.20E-18	(Sander et al., 2011)[*5]	1.00E-19	(Sander et al., 2011)	**0.11**	**0.15**	8.3
Ambient average	-	-	-	-	-		44[*6]

*1: estimate based on quantum chemical calculations. See details below.

*2: extrapolation from the data between 210 and 280 nm, whose logarithm manifests a good linear wavelength-dependence

*3: value at 193 nm

*4: value at 252 nm

*5: linear extrapolation from the data between 196–206 nm

*6: estimated based on i) ambient OH concentration of 1.5×10^6 molecules cm^{-3} (Mao et al., 2009), ii) OH_{exp} of ~2×10^{13} molecules cm^{-3} s in Case HHH (1.8×10^{13} molecules cm^{-3} s for OFR185; 2.3×10^{13} molecules cm^{-3} s for OFR254-70), and iii) average ambient SOA photolysis lifetime of 3.5 d (Hodzic et al., 2015)

Table S8. Number of e-fold decays of photolysis and percentage of photolyzed OA of several SOA samples at an equivalent photochemical age of 1 week under atmospheric conditions in Romonosky et al. (2015a) and in OFR254-70 at 44% relative humidity (water vapor mixing ratio of 1.4%) and 25 s^{-1} initial OHR_{ext}. Absorption cross-sections at 254 nm and effective ambient photolysis lifetimes of SOA samples are taken from or calculated according to Romonosky et al. (2015a). Ambient photolysis data are obtained assuming quantum yields of SOA samples to be those of H_2O_2 or acetone.

SOA type	Cross-section at 254 nm (cm^2)	Effective ambient photolysis lifetime (min)		Number of e-fold decays due to photolysis			Percentage of photolyzed OA at equivalent photochemical age of 1 week		
		Using QY of H_2O_2	Using QY of acetone	OFR254-70	Ambient using QY of H_2O_2	Ambient using QY of acetone	OFR254-70	Ambient using QY of H_2O_2	Ambient using QY of acetone
2-methylpyrrole/O_3	1.66E-17	1	85	0.461	10080	119	36.9	100	100
guaiacol/OH	9.34E-18	1.7	190	0.259	5929	53	22.8	100	100
catechol/O_3	7.97E-18	3	260	0.221	3360	39	19.8	100	100
2-methylpyrrole/OH/NO_x	6.82E-18	1	130	0.189	10080	78	17.2	100	100
p-xylene/OH/NO_x	6.46E-18	2.5	280	0.179	4032	36	16.4	100	100
p-xylene/OH	5.99E-18	5.5	430	0.166	1833	23	15.3	100	100
toluene/OH/NO_x	5.93E-18	1.3	190	0.164	7754	53	15.2	100	100
2-methylpyrrole/OH	5.61E-18	2.6	260	0.155	3877	39	14.4	100	100
naphthalene/OH	4.98E-18	0.62	64	0.138	16258	158	12.9	100	100
toluene/OH	3.42E-18	6.2	590	0.095	1626	17	9.1	100	100
ocimene/OH	2.27E-18	25	1700	0.063	403	5.9	6.1	100	99.7
myrcene/O_3	1.88E-18	58	3800	0.052	174	2.7	5.1	100	93.0
ocimene/OH/NO_x	1.59E-18	25	1800	0.044	403	5.6	4.3	100	99.6
farnesene/OH	1.44E-18	53	3500	0.040	190	2.9	3.9	100	94.4
farnesene/OH/NO_x	1.07E-18	47	3400	0.030	214	3.0	2.9	100	94.8
d-limonene/O_3	5.95E-19	230	7200	0.016	44	1.4	1.6	100	75.3
imidazole/O_3	5.76E-19	95	4800	0.016	106	2.1	1.6	100	87.8
α-pinene/O_3	5.54E-19	85	4800	0.015	119	2.1	1.5	100	87.8

isoprene/OH	5.07E-19	410	7600	0.014	25	1.3	1.4	100	73.5
b-pinene/O_3	4.68E-19	90	4000	0.013	112	2.5	1.3	100	92.0
isoprene/O_3	4.42E-19	88	5400	0.012	115	1.9	1.2	100	84.5
linalool/OH/NO_x	3.65E-19	100	7700	0.010	101	1.3	1.0	100	73.0
linalool/OH	2.92E-19	160	11000	0.008	63	0.9	0.8	100	60.0

Table S9. Estimation equations of $O(^3P)$, $O(^1D)$, and O_3 exposures and ratios of $F254_{exp}$ to OH_{exp} for both OFR185 and OFR254, and ratio of $F185_{exp}$ to OH_{exp} for OFR185. UV in the equations for OFR185 and OFR254 are the photon fluxes at 185 and 254 nm, respectively. Numbers of fitted datapoints and average absolute value of the relative deviations (AAVRD) of the estimates by the equations from the fitted datapoints are also shown. rO_3 is the ratio between O_3 at the reactor exit and entrance. For OFR254, one of rO_3 and UV can be obtained by collectively considering and solving Eqs. 11 and 12 in Peng et al. (2015b) if the other is known. OH, O_3, $O(^1D)$, and $O(^3P)$ exposures are in molecules cm^{-3} s, $F185_{exp}$ and $F254_{exp}$ in photons cm^{-2}, OHR_{ext} in s^{-1}, UV in photons cm^{-2} s^{-1}, $O_{3,in}$ in ppb, and H_2O and rO_3 unitless.

| OFR type	Eq. No.	Estimation equation	Number of fitted datapoints	AAVRD (%)
OFR185	S1	$\log O_{3exp} = 3.1825 + 0.98741 \log UV + 40.352 H_2O - 3.8184 H_2O \cdot \log UV$	28800	6
	S2	$\log O(^3P)_{exp} = 313.61 - 558.66 \log(\log O_{3exp}) - 171.59 H_2O + 254.33(\log(\log O_{3exp}))^2 + 147.27 H_2O \cdot \log(\log O_{3exp})$		6
	S3	$\log O(^1D)_{exp} = 90.595 - 208.28 \log(\log O_{3exp}) - 155.9 H_2O + 114.15(\log(\log O_{3exp}))^2 + 134.4 H_2O \cdot \log(\log O_{3exp})$		4
	S4	$\log(F185_{exp}/OH_{exp}) = -2.7477 - 0.79645 \log H_2O + 0.25018 \log O_{3exp} + 3.8051 \log OHR_{ext} -0.22685 \log OHR_{ext} \cdot \log O_{3exp} + 0.0086381(\log OHR_{ext})^2 \cdot \log O_{3exp}$		14
	S5	$\log(F254_{exp}/OH_{exp}) = 3.325 - 0.8268 \log H_2O + 3.7467 \log OHR_{ext} -0.22294 \log OHR_{ext} \cdot \log O_{3exp} + 0.0086345(\log OHR_{ext})^2 \cdot \log O_{3exp}$		14
OFR254	S6	$\log O_{3exp} = 15.559 + \log O_{3,in} + 0.42073 \log rO_3$	316800	1
	S7	$\log O(^3P)_{exp} = 7.6621 + 0.16135 \log(-\log rO_3) - 1.1342 \log H_2O + 0.59182 \log O_{3,in} - 0.17007 \log H_2O \cdot \log(-\log rO_3) - 0.3797(\log(-\log rO_3))^2 + 0.099902 \log OHR_{ext}$		12
	S8	$\log O(^1D)_{exp} = 3.7371 + 0.1608 \log(-\log rO_3) - 1.1344 \log H_2O + 0.59179 \log O_{3,in} - 0.17019 \log H_2O \cdot \log(-\log rO_3) - 0.37983(\log(-\log rO_3))^2 + 0.099941 \log OHR_{ext}$		12
	S9	$\log(F254_{exp}/OH_{exp}) = 2.8045 - 0.888519 \log H_2O - 0.015648 \log(-\log rO_3) - 0.2607 \log OHR_{ext} -0.1641(\log(-\log rO_3))^2 + (OHR_{ext}/O_{3,in})^{0.25142}$		14
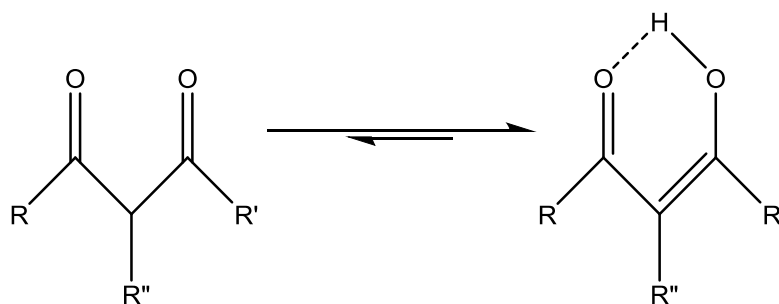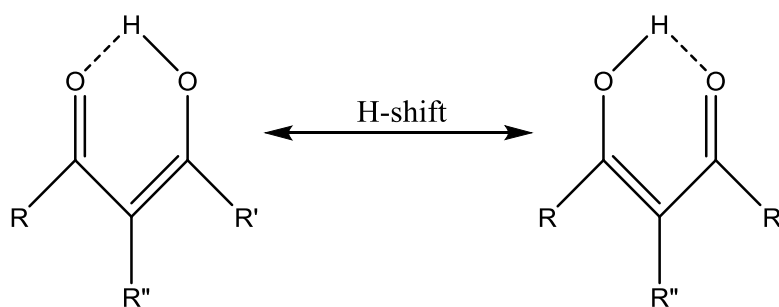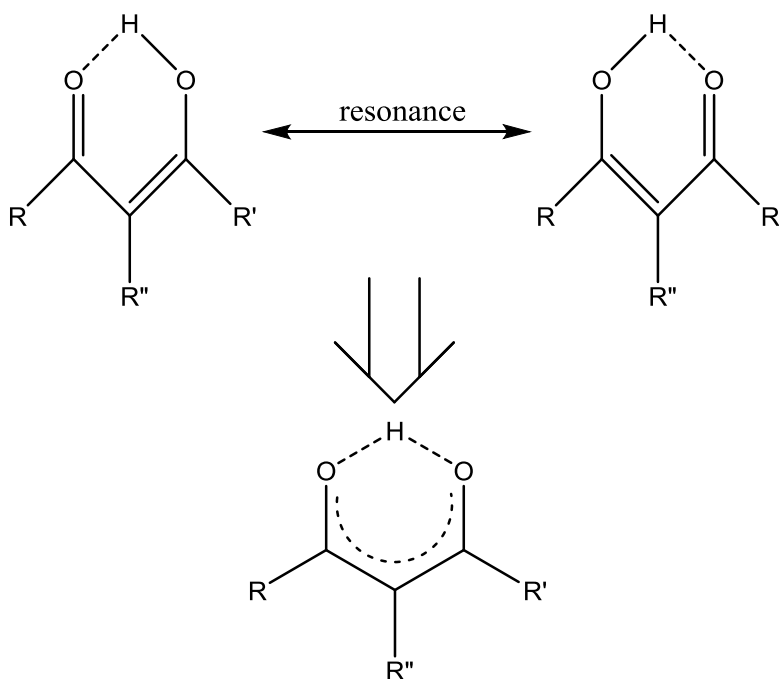
Scheme S1. Keto-enol tautomerism of β-diketone, and H-shift between O atoms or resonance of the enol form. Note that the tautomerism is generally favorable toward the enol form (Burdett and Rogers, 1964) and that the enol form, particularly its resonance, results in an extensive conjugated ring structure, which may have high absorptivity.

S1. Selection of kinetic data

This study involves photoabsorption cross-sections at 185 and 254 nm, rate constants of reactions with OH, $O(^1D)$, $O(^3P)$, and O_3 of a large variety of species of interest. Obviously, we are not able to include all possible reactants. Instead, we include one or two representative species for a category of species with certain functional group(s). The selection of presented species is subject to data availability. In principle, we choose species with available kinetic data to cover categories with different functional groups. However, for example, rate constants of reactions with $O(^1D)$ have seldom been measured. Some categories (e.g., aromatics) are thus not covered. In case of multiple available dataset for a single cross-section/rate constant, we apply the following rules:

    i)   Photoabsorption cross-section data from different sources are used in the priority order of MPI-Mainz UV/VIS Spectral Atlas of Gaseous Molecules of Atmospheric Interest (Keller-Rudek et al., 2015) > JPL Chemical Kinetic Data Evaluation (Sander et al., 2011) > other sources;

    ii)   The latest dataset is selected in case of multiple available references in MPI-Mainz UV/VIS Spectral Atlas of Gaseous Molecules of Atmospheric Interest;

    iii)   Data of rate constants of thermal reactions from different sources are used in the priority order of Atkinson and Arey (2003) > JPL Chemical Kinetic Data Evaluation (Sander et al., 2011) > IUPAC Task Group on Atmospheric Chemical Kinetic Data Evaluation (Ammann et al., 2015) > other sources.

In some cases, kinetic data are also collected under certain reliable approximations, despite no available direct measurements. For example, to obtain cross-section of methylhydroperoxide at 185 nm, we make an extrapolation from the data between 210 and 280 nm, whose logarithm manifests a good linear wavelength-dependence; we use cross-section of ethyl acetate at 252 nm as that at 254 nm.

According to data in Trost et al. (1997) and Atkinson and Arey (2003), photolysis of benzaldehydes and phenols at 254 nm is significant compared to their reactions with OH. It is important to assess their photolysis at 185 nm. However, no measured cross-section data are available. Moreover, no appropriate assumptions based on available data to obtain cross-sections at 185 nm can be made. We thus make an estimation of these cross-sections based on quantum chemical calculations.

S2. Estimation of 185 nm absorption cross-sections of several aromatics

We perform time-dependent density functional theory calculations (Runge and Gross, 1984) using GAMESS program (Schmidt et al., 1993) for the molecule of interest: ground state geometry is optimized at Perdew-Burke-Ernzerhof0/6-311g(d,p) level (Perdew et al., 1996). Oscillator strengths of transitions between 160 and 300 nm are obtained by time-dependent calculations at the same level with the first 10 excited states considered. Then cross-section at 185 nm is estimated under the assumption that the ratio between cross-sections at 185 nm and absorption maximum wavelength in the longer-wavelength range, where experimental data are available in Keller-Rudek et al. (2015), is equal to that between oscillator strengths of transitions closest to 185 nm and absorption maximum wavelength, respectively. This is a very rough approximation completely neglecting vibronic structure of absorption bands. However, in this study, we only seek cross-section values on the right order of magnitude, but not quantum chemical predictions quantitatively comparable to measurements, which require vibrational/vibronic wavefunctions of dissociative excited states and are far beyond this work's scope.

The main features that we find from theoretical estimates, i.e., estimated 185 nm cross-sections are around 10^{16} cm^2/molecule and 2 orders of magnitude larger than those at 254 nm, agree well with the available data for other aromatics, i.e., toluene and p-xylene (Table S1).

S3. Estimation equations of non-OH reactant exposures

In order that one may practically estimate exposure ratios between non-OH reactants and OH under any condition for OFR operation, we provide the estimation equations of $O(^3P)$, $O(^1D)$, and O_3 exposures obtained by fitting the modeling results (Table S9). The equations for OFR254 are

fitted from the results of the same runs as in Peng et al. (2015b), while those for OFR185 from the modeling data under conditions spanning the same H$_2$O, UV, and OHR$_{ext}$ ranges as for OFR254, but without the initial O$_3$ (O$_{3,in}$) dimension. Exposures estimated from these equations compare very well with the modeled exposures (Fig. S6). Scatter plots between a few exposures are also shown in Fig. S6.

For OFR254, UV at 254 nm can be estimated by collectively considering and solving Eqs. 11 and 12 in Peng et al. (2015b), if rO$_3$ (i.e., ratio between O$_3$ at the reactor entrance and exit) is known, and vice versa. For OFR185, one of UV at 185 nm and O$_{3exp}$ (or average O$_3$) can be obtained if the other is known according to Eq. S1 below. UV at 254 nm in OFR185 can be calculated by Eq. S1 in Li et al. (2015), and then photon flux exposures can be easily estimated.

The ratios of F185 and F254 exposures to OH exposure are the most important parameter in this work that determine the relative contribution of non-tropospheric VOC photolysis. Therefore, we also provide equations for directly estimating these parameters from measurable surrogates of UV (i.e., O$_{3exp}$ in OFR185 and rO$_3$ in OFR254) (Table S9 and Fig. S6).

References

Ammann, M., Cox, R. A., Crowley, J. N., Jenkin, M. E., Mellouki, A., Rossi, M. J., Troe, J., Wallington, T. J., Cox, B., Atkinson, R., Baulch, D. L. and Kerr, J. A.: IUPAC Task Group on Atmospheric Chemical Kinetic Data Evaluation, [online] Available from: http://iupac.pole-ether.fr/#, 2015.

Atkinson, R.: Kinetics and mechanisms of the gas-phase reactions of the hydroxyl radical with organic compounds under atmospheric conditions, Chem. Rev., 86(1), 69–201, doi:10.1021/cr00071a004, 1986.

Atkinson, R. and Arey, J.: Atmospheric degradation of volatile organic compounds., Chem. Rev., 103(12), 4605–38, doi:10.1021/cr0206420, 2003.

Atkinson, R., Baulch, D. L., Cox, R. A., Hampson, R. F., Kerr, J. A., Rossi, M. J. and Troe, J.: Evaluated Kinetic and Photochemical Data for Atmospheric Chemistry: Supplement VI. IUPAC Subcommittee on Gas Kinetic Data Evaluation for Atmospheric Chemistry, J. Phys. Chem. Ref. Data, 26(6), 1329, doi:10.1063/1.556010, 1997.

Baulch, D. L., Cobos, C. J., Cox, R. A., Frank, P., Hayman, G., Just, T., Kerr, J. A., Murrells, T., Pilling, M. J., Troe, J., Walker, R. W. and Warnatz, J.: Evaluated Kinetic Data for Combustion Modeling. Supplement I, J. Phys. Chem. Ref. Data, 23(6), 847, doi:10.1063/1.555953, 1994.

Borbon, A., Gilman, J. B., Kuster, W. C., Grand, N., Chevaillier, S., Colomb, A., Dolgorouky, C., Gros, V., Lopez, M., Sarda-Esteve, R., Holloway, J., Stutz, J., Petetin, H., McKeen, S., Beekmann, M., Warneke, C., Parrish, D. D. and De Gouw, J. A.: Emission ratios of anthropogenic volatile organic compounds in northern mid-latitude megacities: Observations versus emission inventories in Los Angeles and Paris, J. Geophys. Res. Atmos., 118(4), 2041–2057, doi:10.1002/jgrd.50059, 2013.

El Boudali, A., Le Calvé, S., Le Bras, G. and Mellouki, A.: Kinetic Studies of OH Reactions with a Series of Acetates, J. Phys. Chem., 10(30), 12364–12368, doi:10.1021/jp9606218, 1996.

Burdett, J. L. and Rogers, M. T.: Keto-Enol Tautomerism in β-Dicarbonyls Studied by Nuclear Magnetic Resonance Spectroscopy. 1 I. Proton Chemical Shifts and Equilibrium Constants of Pure Compounds, J. Am. Chem. Soc., 86(11), 2105–2109, doi:10.1021/ja01065a003, 1964.

Chen, Z. and Wang, C.: Rate constants of the gas-phase reactions of CH3OOH with O3 and NOx at 293K, Chem. Phys. Lett., 424(4-6), 233–238, doi:10.1016/j.cplett.2006.04.026, 2006.

Cohen, N. and Westberg, K. R.: Chemical Kinetic Data Sheets for High-Temperature Reactions. Part II, J. Phys. Chem. Ref. Data, 20(6), 1211, doi:10.1063/1.555901, 1991.

Cvetanović, R. J.: Evaluated Chemical Kinetic Data for the Reactions of Atomic Oxygen O(3P) with Unsaturated Hydrocarbons, J. Phys. Chem. Ref. Data, 16(2), 261, doi:10.1063/1.555783, 1987.

Dillon, T. J., Horowitz, A. and Crowley, J. N.: The atmospheric chemistry of sulphuryl fluoride, SO2F2, Atmos. Chem. Phys., 8(6), 1547–1557, doi:10.5194/acp-8-1547-2008, 2008.

Ferguson, J., Reeves, L. W. and Schneider, W. G.: VAPOR ABSORPTION SPECTRA AND OSCILLATOR STRENGTHS OF NAPHTHALENE, ANTHRACENE, AND PYRENE, Can. J. Chem., 35(10), 1117–1136, doi:10.1139/v57-152, 1957.

Foster, R.: Organic Charge-Transfer Complexes, Academic Press, New York., 1969.

Frerichs, H., Tappe, M. and Wagner, H. G.: Comparison of the Reactions of Mono- and Polycyclic Aromatic Hydrocarbons with Oxygen Atoms, Berichte der Bunsengesellschaft für Phys. Chemie, 94(11), 1404–1407, doi:10.1002/bbpc.199000043, 1990.

Halasinski, T. M., Salama, F. and Allamandola, L. J.: Investigation of the Ultraviolet, Visible, and Near-Infrared Absorption Spectra of Hydrogenated Polycyclic Aromatic Hydrocarbons and Their Cations, Astrophys. J., 628(1), 555–566, doi:10.1086/430631, 2005.

Herron, J. T.: Evaluated Chemical Kinetic Data for the Reaction of Atomic Oxygen, O(3P), with Saturated Organic Compounds in the Gas Phase, J. Phys. Chem. Ref. Data., 17(3), 967–994, doi:10.1063/1.555810, 1988.

Hodzic, A., Madronich, S., Kasibhatla, P. S., Tyndall, G., Aumont, B., Jimenez, J. L., Lee-Taylor, J. and Orlando, J.: Organic photolysis reactions in tropospheric aerosols: effect on secondary organic aerosol formation and lifetime, Atmos. Chem. Phys., 15(16), 9253–9269, doi:10.5194/acp-15-9253-2015, 2015.

Kajimoto, O. and Fueno, T.: Relative rate constants of O(1D2)—olefin reactions, Chem. Phys. Lett., 64(3), 445–447, doi:10.1016/0009-2614(79)80218-3, 1979.

Keller-Rudek, H., Moortgat, G. K., Sander, R. and Sörensen, R.: The MPI-Mainz UV/VIS Spectral Atlas of Gaseous Molecules of Atmospheric Interest, [online] Available from: www.uv-vis-spectral-atlas-mainz.org, 2015.

Li, R., Palm, B. B., Ortega, A. M., Hu, W., Peng, Z., Day, D. A., Knote, C., Brune, W. H., de Gouw, J. and Jimenez, J. L.: Modeling the radical chemistry in an Oxidation Flow Reactor (OFR): radical formation and recycling, sensitivities, and OH exposure estimation equation, J. Phys. Chem. A, 119(19), 4418–4432, doi:10.1021/jp509534k, 2015.

Luo, D., Pierce, J. A., Malkina, I. L. and Carter, W. P. L.: Rate constants for the reactions of O(3P) with selected monoterpenes, Int. J. Chem. Kinet., 28(1), 1–8, doi:10.1002/(SICI)1097-4601(1996)28:1<1::AID-KIN1>3.0.CO;2-Z, 1996.

Mao, J., Ren, X., Brune, W. H., Olson, J. R., Crawford, J. H., Fried, a., Huey, L. G., Cohen, R. C., Heikes, B., Singh, H. B., Blake, D. R., Sachse, G. W., Diskin, G. S., Hall, S. R. and Shetter, R. E.: Airborne measurement of OH reactivity during INTEX-B, Atmos. Chem. Phys., 9(1), 163–173, doi:10.5194/acp-9-163-2009, 2009.

Mellouki, A. and Mu, Y.: On the atmospheric degradation of pyruvic acid in the gas phase, J. Photochem. Photobiol. A Chem., 157(2-3), 295–300, doi:10.1016/S1010-6030(03)00070-4, 2003.

Messaadia, L., El Dib, G., Ferhati, A. and Chakir, A.: UV–visible spectra and gas-phase rate coefficients for the reaction of 2,3-pentanedione and 2,4-pentanedione with OH radicals, Chem. Phys. Lett., 626, 73–79, doi:10.1016/j.cplett.2015.02.032, 2015.

Michaud, P., Paraskevopoulos, G. and Cvetanovic, R. J.: Relative rates of the reactions of O(1D2) atoms with alkanes and cycloalkanes, J. Phys. Chem., 78(15), 1457–1461, doi:10.1021/j100608a003, 1974.

Peng, Z., Day, D. A., Stark, H., Li, R., Lee-Taylor, J., Palm, B. B., Brune, W. H. and Jimenez, J. L.: HOx radical chemistry in oxidation flow reactors with low-pressure mercury lamps systematically examined by modeling, Atmos. Meas. Tech., 8(11), 4863–4890, doi:10.5194/amt-8-4863-2015, 2015.

Perdew, J. P., Burke, K. and Ernzerhof, M.: Generalized Gradient Approximation Made Simple, Phys. Rev. Lett., 77(18), 3865–3868, doi:10.1103/PhysRevLett.77.3865, 1996.

Pitts, J. N., Sandoval, H. L. and Atkinson, R.: Relative rate constants for the reaction of O(1D) atoms with fluorocarbons and N2O, Chem. Phys. Lett., 29(1), 31–34, doi:10.1016/0009-2614(74)80129-6, 1974.

Romonosky, D. E., Ali, N. N., Saiduddin, M. N., Wu, M., Lee, H. J. (Julie), Aiona, P. K. and Nizkorodov, S. A.: Effective absorption cross sections and photolysis rates of anthropogenic and biogenic secondary organic aerosols, Atmos. Environ., 130, 172–179, doi:10.1016/j.atmosenv.2015.10.019, 2016.

Runge, E. and Gross, E. K. U.: Density-functional theory for time-dependent systems, Phys. Rev. Lett., 52(12), 997–1000, doi:10.1103/PhysRevLett.52.997, 1984.

Salter, L. F. and Thrush, B. A.: Reaction of oxygen atoms with methyl and ethyl nitrates, J. Chem. Soc. Faraday Trans. 1, 73, 1098, doi:10.1039/f19777301098, 1977.

Sander, S. P., Friedl, R. R., Barker, J. R., Golden, D. M., Kurylo, M. J., Wine, P. H., Abbatt, J. P. D., Burkholder, J. B., Kolb, C. E., Moortgat, G. K., Huie, R. E. and Orkin, V. L.: Chemical Kinetics and Photochemical Data for Use in Atmospheric Studies Evaluation Number 17, Pasadena, CA, USA. [online] Available from: http://jpldataeval.jpl.nasa.gov/pdf/JPL%10-6%Final%15June2011.pdf, 2011.

Schmidt, M. W., Baldridge, K. K., Boatz, J. A., Elbert, S. T., Gordon, M. S., Jensen, J. H., Koseki, S., Matsunaga, N., Nguyen, K. A., Su, S., Windus, T. L., Dupuis, M. and Montgomery, J. A.: General atomic and molecular electronic structure system, J. Comput. Chem., 14(11), 1347–1363, doi:10.1002/jcc.540141112, 1993.

Schubert, C. C., Schubert, S. and Pease, R. N.: The Oxidation of Lower Paraffin Hydrocarbons. I. Room Temperature Reaction of Methane, Propane, n-Butane and Isobutane with Ozonized Oxygen 1, J. Am. Chem. Soc., 78(10), 2044–2048, doi:10.1021/ja01591a006, 1956.

Toby, S., Van de Burgt, L. J. and Toby, F. S.: Kinetics and chemiluminescence of ozone-aromatic reactions in the gas phase, J. Phys. Chem., 89(10), 1982–1986, doi:10.1021/j100256a034, 1985.

Trost, B., Stutz, J. and Platt, U.: UV-absorption cross sections of a series of monocyclic aromatic compounds, Atmos. Environ., 31(23), 3999–4008, doi:10.1016/S1352-2310(97)00214-8, 1997.

Tsalkani, N., Mellouki,   a., Poulet, G., Toupance, G. and Bras, G.: Rate constant measurement for the reactions of OH and Cl with peroxyacetyl nitrate at 298 K, J. Atmos. Chem., 7(4), 409–419, doi:10.1007/BF00058713, 1988.

Wolfe, G. M., Crounse, J. D., Parrish, J. D., St. Clair, J. M., Beaver, M. R., Paulot, F., Yoon, T. P., Wennberg, P. O. and Keutsch, F. N.: Photolysis, OH reactivity and ozone reactivity of a proxy for isoprene-derived hydroperoxyenals (HPALDs), Phys. Chem. Chem. Phys., 14(20), 7276, doi:10.1039/c2cp40388a, 2012.

Ziemann, P. and Atkinson, R.: Kinetics, products, and mechanisms of secondary organic aerosol formation, Chem. Soc. Rev., 41(19), 6582, doi:10.1039/c2cs35122f, 2012.